

Effect of metal cations on the photochromic properties of spironaphthoxazines conjugated with aza-15(18)-crown-5(6) ethers

Olga A. Fedorova,^{*a} Yuri P. Strokach,^a Sergey P. Gromov,^a Alexander V. Koshkin,^a Tatjana M. Valova,^a Michael V. Alfimov,^a Alexei V. Feofanov,^b Iouri S. Alaverdian,^b Vladimir A. Lokshin,^c Andre Samat,^c Robert Guglielmetti,^c Reuben B. Girling,^d John N. Moore^d and Ronald E. Hester^d

^a Center of Photochemistry at the Joint N. N. Semenov Institute of Chemical Physics of the Russian Academy of Sciences, ul. Novatorov 7a, 117421 Moscow, Russia.

E-mail: fedorova@photonics.ru

^b Shemyakin-Ovchinnikov Institute of Bioorganic Chemistry, Russian Academy of Sciences, ul. Miklukho-Maklaya 16/10, 117997 Moscow, Russia

^c Laboratoire de Photochimie Organique Appliquée (CNRS UMR 6114), Faculté des Sciences de Luminy, Case 901, Université de la Méditerranée, 13288 Marseille cedex 9, France

^d Department of Chemistry, University of York, Heslington, York, YO10 5DD, UK

Received (in Montpellier, France) 22nd January 2002, Accepted 26th March 2002

First published as an Advance Article on the web 29th July 2002

Spironaphthoxazines conjugated with aza-15(18)-crown-5(6)-ether moieties at the 6'-position of the naphthalene fragment (crown-containing spironaphthoxazine, CSN) were synthesised and studied for the first time. The addition of Li⁺ and alkaline earth (Mg²⁺, Ca²⁺, Sr²⁺ and Ba²⁺) metal cations to CSN solutions results in a hypsochromic shift of the UV absorption band of the spiro form and a bathochromic shift of the absorption band of the merocyanine form in the visible region. In addition, the equilibrium shifts to the merocyanine form, and the lifetime of the photoinduced merocyanine form increases. Analysis of the spectral and kinetic data allows a complexation scheme to be proposed and the stability constants of the resulting complexes to be calculated. According to the results obtained, the complexation with Li⁺ and alkaline earth metal cations in acetonitrile initially involves the crown ether moiety; the participation of the merocyanine oxygen atom in the complexation process occurs at a high metal cation concentration. The UV-induced isomerisation of CSN into the merocyanine form causes a decrease of the cation binding ability.

Photochromic compounds can exist in two or more stable states with different spectral characteristics.^{1–3} The equilibrium between these states can be shifted either by UV or visible-light irradiation or by changing the parameters of the medium. In addition, photochromic compounds containing ionophoric fragments are able to react with metal cations; in some cases this can also change the spectral characteristics of the photochromic ligands.^{4–8} Compounds of this type provide the possibility of monitoring the presence of metal ions in solutions; they are of considerable interest in developing efficient ionophores for selective determination of metal ions.

Previously, photochromic ionophores containing crown ether fragments located at different positions of spironaphthoxazine and linked to the main molecular cage by methylene bridges of various lengths have been synthesised and investigated.^{9–12} It was demonstrated that the influence of metal ions on the spectral and photochemical properties of these compounds is enhanced due to a direct structure-assisted interaction between the oxygen atom of the merocyanine form (MF) and the metal cation located in the crown ether cavity. Efficient coordination between the merocyanine oxygen and the “crowned” metal cation and, finally, considerable stabilisation of MF were achieved by optimising the length of the methylene chain.

In order to develop spironaphthoxazine-based systems that are more sensitive to the presence of metal cations in solutions than those known previously, we synthesised and studied for

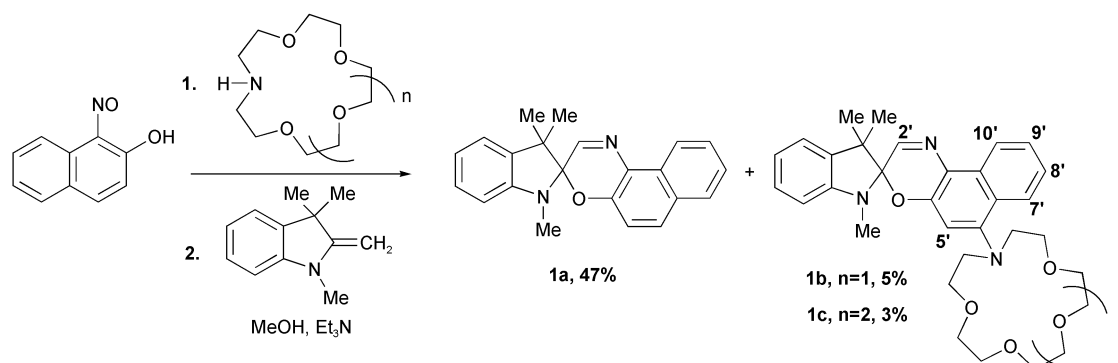
the first time spironaphthoxazines **1b,c** (CSN) with conjugated azacrown ether fragments (Scheme 1). The parent spironaphthoxazine **1a** (SN) was used for comparison.

Results and discussion

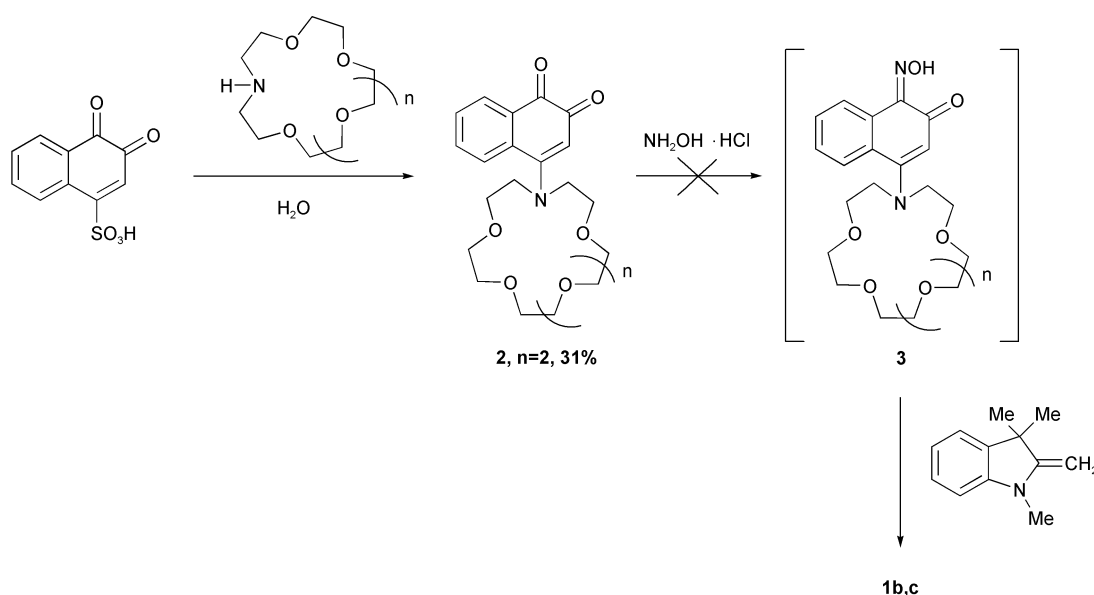
Synthesis

The CSN **1b,c** were synthesised using to the methods developed for the synthesis of 6'-amino-substituted spironaphthoxazines by Rickwood *et al.*¹³ Scheme 1 outlines these methods as applied to compounds **1b,c**. The researchers cited found that 6'-aminospironaphthoxazines of various structures can be prepared by condensation of 2-methyleneindolenine with 4-amino-1-nitroso-2-naphthol. The latter compound is prepared by nucleophilic substitution of a secondary amine for the 4-hydrogen atom in 1-nitroso-2-naphthol (method A) or *via* a two-step procedure (method B) from sodium 1,2-naphthoquinone-4-sulfonate. Method A was employed¹³ to synthesise spironaphthoxazines containing dimethylamine, piperidine or morpholine residues as substituents at the 6'-position of SN. The product yields were moderate (0.5 to 20%); however, both steps were performed successively in one flask without isolation of intermediates. Method B implies the isolation of products at each intermediate step; the yield of similar products with this procedure reached 50%.

Method A



Method B



Scheme 1

We have tested both methods for the synthesis of CSN **1b,c**. In method B, the 1,2-naphthoquinone derivative **2** was isolated in the first step. However, subsequently, we were unable to select appropriate conditions for the reaction of **2** with hydroxylamine to give crown-containing 1-nitroso-2-naphthol (**3**).

The reaction of 1-nitroso-2-naphthol with aza-15(18)-crown-5(6) ethers followed by the reaction with indolenine was carried out in ethanol in the presence of Et₃N. The yields were relatively low, namely, 5% (**1b**) and 3% (**1c**); variation of the reaction conditions (temperature, reactant ratio, and duration) did not increase the yield of the target product. The unsubstituted SN **1a** was formed as a side product.

Spectral properties of CSN **1b,c** and their complexes with metal cations

UV-VIS absorption study. It is known² that both spiro form (SF) and MF of a spironaphthoxazine molecule co-exist in equilibrium in solution. The absorption spectrum of SN **1a** in MeCN exhibits virtually no bands related to MF, and SF dominates in solution. This indicates that the mutual arrangement of the ground-state energy levels of SF and MF of SN **1a** does not provide an appreciable thermal occupancy of the ground state of MF.

The introduction of the azacrown ether fragment into the 6'-position of the naphthalene nucleus of SN induces a

bathochromic shift of the absorption band of SF (12 nm, Table 1). In addition, it gives rise to a weak absorption band of MF in the visible region, which is blue shifted *ca.* 28 nm as compared to the band of photoinduced MF of spironaphthoxazine **1a** (Table 1). This indicates that the azacrown fragment displaces the equilibrium slightly towards MF. The observed spectral shift of MF absorption is due to the electron-donating effect of the azacrown ether moiety conjugated with the π -electron system of the molecule. Similar spectral changes have been found previously for spironaphthoxazines containing electron-donating substituents such as morpholine or piperidine residues at the 6'-position.¹⁴

Addition of metal cations into solutions of CSN **1b,c** results in changes of the absorption spectra of the molecules that point to a metal-ligand interaction. The full scheme of feasible thermodynamic equilibrium states of CSN **1b,c** in the presence of metal cations should include two probable sites of complex formation (Scheme 2).

At low metal/ligand molar ratios (C_M/C_L) the spectral changes occur in the UV region only. They include a small hypsochromic shift (1–5 nm, Table 1) and an intensity decrease of the 380 nm absorption band (Fig. 1). These spectral changes were observed distinctly for all the studied metal cations (Li⁺, Ba²⁺, Mg²⁺, Ca²⁺ and Sr²⁺). Specific alterations in the UV region occurring in the absence of MF related changes in the visible range allow one to conclude that a complex forms between a crown ether moiety of SF and a metal cation, M^{*n*+}

Table 1 Photochromic characteristics of spironaphthoxazines **1a–c** and their complexes with alkali (Li^+) and alkaline earth (Mg^{2+} , Ca^{2+} , Sr^{2+} , Ba^{2+}) metal ions in acetonitrile

Compound ^a	$\lambda_{\text{SF}}^b/\text{nm}$ ($\epsilon_{\text{SF}} \times 10^{-4}/\text{mol}^{-1}\text{cm}^{-1}$)	$\lambda_{\text{MF}}^c/\text{nm}$ ($\epsilon_{\text{MF}} \times 10^{-4}/\text{mol}^{-1}\text{cm}^{-1}$)	$k_{\text{MF} \rightarrow \text{SF}}^d/\text{s}^{-1}$
1a	355 (0.56)	593	1.6
1b	367 (1.17)	565 (~0.02)	9.7
1b · Li^+	359	580 (0.03)	7.7
1b · Mg^{2+}	365	605 (0.42)	1.20
1b · Ca^{2+}	350	585 (0.10)	1.19
1b · Sr^{2+}	350	582 (0.05)	3.35
1b · Ba^{2+}	352	575 (0.03)	5.12
1c	367 (1.20)	565 (~0.02)	9.4
1c · Li^+	362	587 (0.03)	8.7
1c · Mg^{2+}	360	606 (0.11)	0.83
1c · Ca^{2+}	360	595 (0.38)	2.16
1c · Sr^{2+}	352	592 (0.22)	0.80
1c · Ba^{2+}	352	590 (0.032)	0.79

^a $C_{\text{L}} = 2 \times 10^{-4} \text{ mol l}^{-1}$, $C_{\text{M}}/C_{\text{L}} = 100$, 24°C . ^b λ_{SF} and ϵ_{SF} are the position and extinction coefficient of the long-wavelength absorption band of SF and its complexes. ^c λ_{MF} and ϵ_{MF} are the maximum and extinction coefficient of the long-wavelength absorption band of free MF and its complexes with metal cations. ^d $k_{\text{MF} \rightarrow \text{SF}}$ is the rate constant for thermal relaxation of free MF and its complexes with metal cations.

(complex **D**, Scheme 2). Beside the oxygen atoms, the nitrogen atom of the crown ether fragment participates in the binding of the metal cation, which decreases its conjugation with the chromophore system. This lowers the electron-donating effect of the azacrown ether moiety, thus inducing a hypsochromic shift of the absorption band of SF.

Since addition of Li^+ , Ba^{2+} , Sr^{2+} or Ca^{2+} cations in the solutions of CSN **1b,c** and Mg^{2+} cations in the CSN **1c** solution does not induce a noticeable SF to MF transition for $C_{\text{M}}/C_{\text{L}}$ molar ratios ranging from 1 to 10, the interaction of

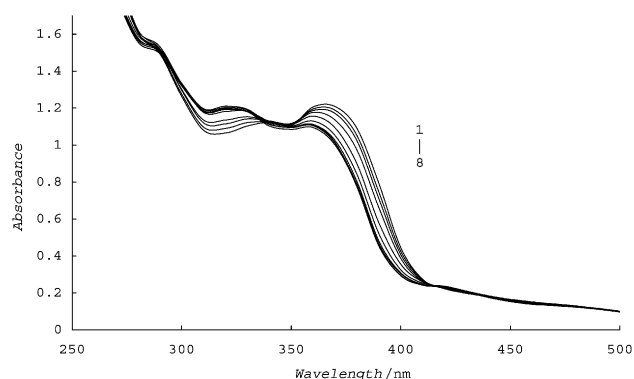


Fig. 1 Changes in the absorption spectra of CSN**1b** in MeCN upon the addition of LiClO_4 (the spectrum of the complex ($\text{Li}^+\cdot\text{1b}$) minus the spectrum of free **1b** at $C_{\text{M}}/C_{\text{L}} = 0.5$ (1); 1 (2); 2 (3); 5 (4); 10 (5); 20 (6); 50 (7); 100 (8).

CSN **1b,c** with metal cations could be described by the simplified equilibrium between states **A** and **D** (Scheme 2), disregarding MF and its complexes under these conditions:

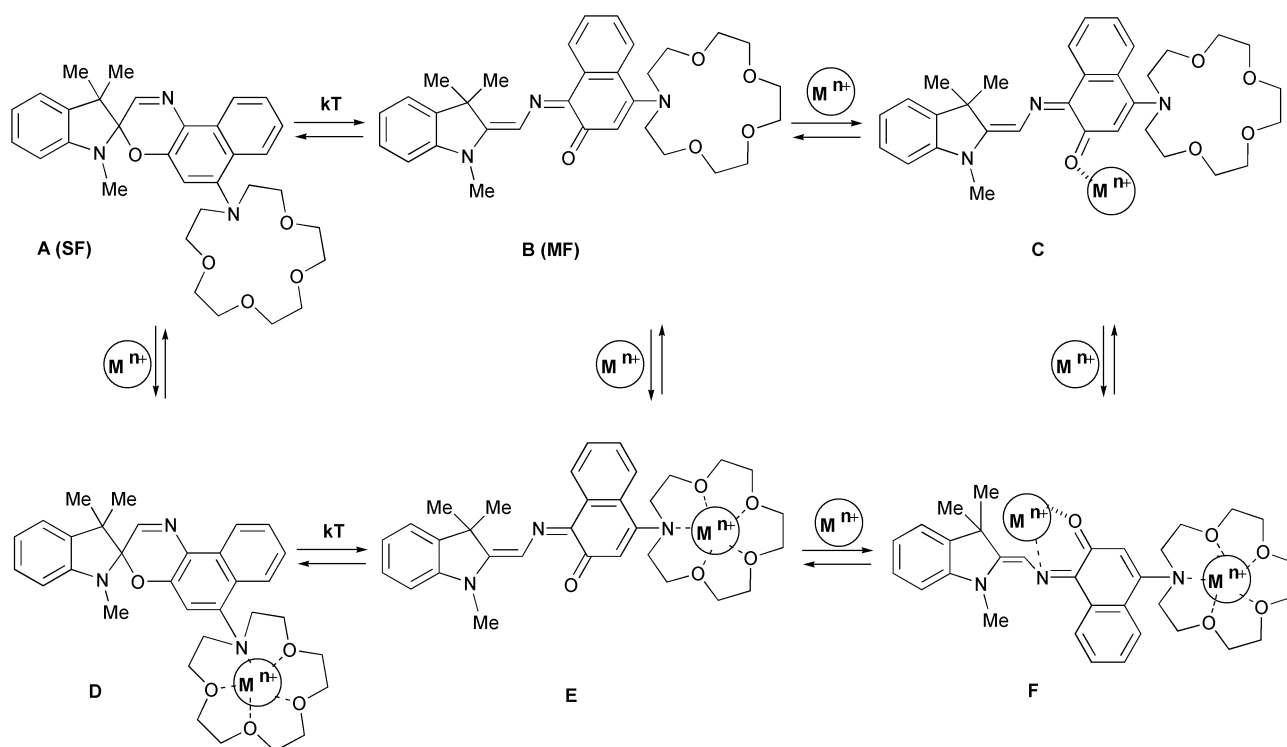


where $[\text{L}]$, $[\text{M}]$ and $[\text{LM}]$ are concentrations of the free ligand, free metal ion, and the complex, respectively; K_{D} is stability constant of the **D** complex.

The cation-induced changes in the UV region of the absorption spectrum can be used to determine K_{D} by spectrophotometric titration. According to eqn (1), the extent of complexation (α) depends on the concentration of metal ions in solution as follows:¹⁵

$$\alpha = (A - A_0)/(A_\infty - A_0) = (C_{\text{L}} + C_{\text{M}} + 1/K_{\text{D}}) \times \{1 - [1 - 4C_{\text{L}}C_{\text{M}}/(C_{\text{L}} + C_{\text{M}} + 1/K_{\text{D}})^2]^{1/2}\}/2C_{\text{L}}, \quad (2)$$

where A_0 is the absorbance of free CSN **1b,c** at 380 nm at the concentration C_{L} , A is the absorbance at 380 nm when metal ions are present at a given concentration C_{M} , and A_∞ is the



Scheme 2

absorbance at the concentration of metal ions that ensures the maximum complexation.

Calculated K_D constants for the complexes of CSN **1b,c** with metal cations are presented in Table 2. The theoretical $\alpha(C_M)$ dependencies derived from eqn (2) with the calculated K_D values and plotted in the $\log \alpha$ vs. $\log (C_M/C_L)$ coordinates are in agreement with the experimental titration data (Fig. 2). This indicates that the complexes formed by SF of the dyes and the studied cations actually have a 1 : 1 stoichiometry for C_M/C_L molar ratios ranging from 1 to 10.

The stability constants of the complexes of CSN **1b** with doubly charged metal cations increase in the order $Ba^{2+} < Sr^{2+} < Ca^{2+}$ in parallel with the decrease in the ion diameter¹⁶ (Table 2). The higher K_D constant of the CSN **1b** complex with Ca^{2+} is, evidently, due to the better correspondence of the cation diameter to the size of the aza-15-crown-5 cavity (1.7–2.2 Å)¹⁷ as compared to that of Sr^{2+} or Ba^{2+} cations. Accordingly, the increased size of the aza-18-crown-6 cavity of CSN **1c** improves considerably the binding of Ca^{2+} and Ba^{2+} cations (Table 2). The stability constants of the CSN **1b** complex with Li^+ and the CSN **1c** complex with Mg^{2+} are low because the cations seem to be too small for an effective complexation with the corresponding azacrown ether cycles.

As the C_M/C_L ratio increases considerably, the MF related absorption band of CSN **1b,c** in the 550–650 nm region (Fig. 3). The interaction of the second metal cation with CSN **1b,c** is assumed to be responsible for MF stabilisation, because MF appears at high C_M/C_L ratios, when cation binding with the azacrown ether cycle approaches saturation for most of the studied metals. This stabilisation corresponds to the formation of complex **F** (in Scheme 2), which has its maximum shifted to

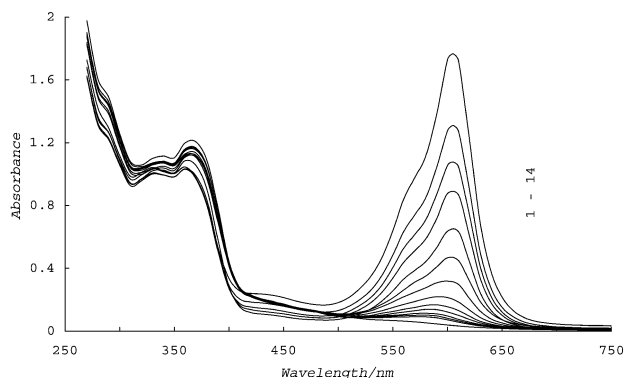


Fig. 3 Absorption spectra of CSN **1b** in MeCN in the presence of $Mg(ClO_4)_2$ in solution [$C_M/C_L = 0$ (1); 0.5 (2); 1 (3); 2 (4); 5 (5); 10 (6); 20 (7); 50 (8); 100 (9); 200 (10); 500 (11); 1000 (12); 2000 (13); 4000 (14)].

longer wavelengths in comparison with that of free MF (**B** in Scheme 2) (Table 1).

It is of interest that the extent of **F** complex formation, estimated qualitatively by the intensity of the **F** absorption band at fixed C_M/C_L ratio (Table 1), depends obviously on the features of the initial interaction between the metal cation and azacrown ether ring. Binding of divalent cations, which fit exactly the size of the azacrown ether cycle (Mg^{2+} and CSN **1b**, Ca^{2+} and CSN **1c**), enhance sharply the formation of the **F** complex. Large Ba^{2+} and Sr^{2+} cations that bind above the plane of the azacrown ether moiety stimulate only weakly the formation of the **F** complex with CSN **1b**, but do this more strongly with CSN **1c**. Considering Li^+ cations, that also fit well in the azacrown ether ring of CSN **1b**, but do not provide the same effect as Mg^{2+} cations, one can conclude that the charge value is also important for **F** complex stabilisation.

NMR study of CSN 1b and its complexes with metal cations. The formation of complexes of CSN **1b** with metal cations was also studied using NMR spectroscopy. The addition of alkaline earth metal perchlorates to a solution of CSN **1b** induces downfield shifts of many proton signals as well as upfield shifts of the signals of the C-5' proton in the case of Mg^{2+} cation and the C-7' proton in the case of Sr^{2+} and Ba^{2+} cations (Table 3). The set of proton signals of the azacrown ether NCH_2 and OCH_2 groups undergoes noticeable alterations, clearly pointing to the interaction of the crown ether moiety with the studied cations. Besides, considerable shifts were observed for the protons of the naphthalene ring (Table 3), but not for those of the benzene ring of the indoline moiety (not shown). It is known² that the indoline and naphthoxazine moieties are approximately orthogonal to each other; this is why the radius of influence of complex formation is limited and signals of the indoline protons are weakly affected. Shifts of the naphthalene ring protons can be due to the following two processes that accompany the complexation. First, the participation of the lone electron pair of nitrogen in the formation of a coordination bond with the metal cation decreases the nitrogen conjugation with the chromophore system and affect in this way the electronic system of the naphthoxazine fragment. Second, the conformation of the naphthoxazine fragment can change upon conformational rearrangement of the macrocycle caused by complexation. According to the results of an X-ray diffraction study,² the conformation of the naphthoxazine fragment is very flexible and is dictated by steric factors in the molecule rather than by electronic effects of the substituents.

No signals related to the MF complex with Ba^{2+} or Sr^{2+} cations are detected with the conditions used. In contrast, the appearance of the MF complex is observed at a substantial

Table 2 Stability constants^a of spironaphthoxazine **1a–c** complexes with alkali and alkaline earth metal cations in acetonitrile

M^{n+}	Cation diameter ^b /Å	1a log K_C	1b		1c	
			log K_D	log K_F	log K_D	log K_F
Li^+	1.36		3.28			
Mg^{2+}	1.32				2.2	
Ca^{2+}	1.98	2.2	3.65	2.4	4.6	2.3
Sr^{2+}	2.24		3.22			
Ba^{2+}	2.68		3.10		5.6	

^a The error of determination of the stability constants of the complexes is $\sim \pm 0.1$. ^b According to the data in ref. 16.

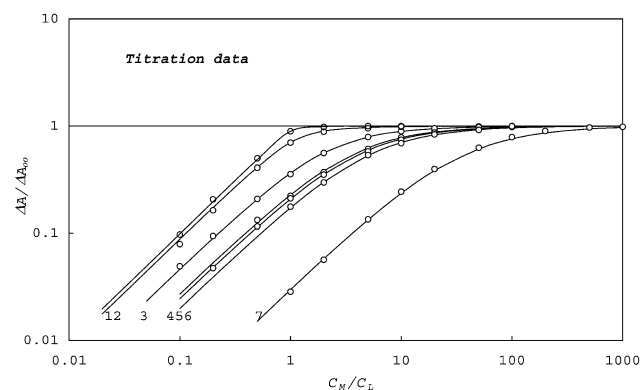
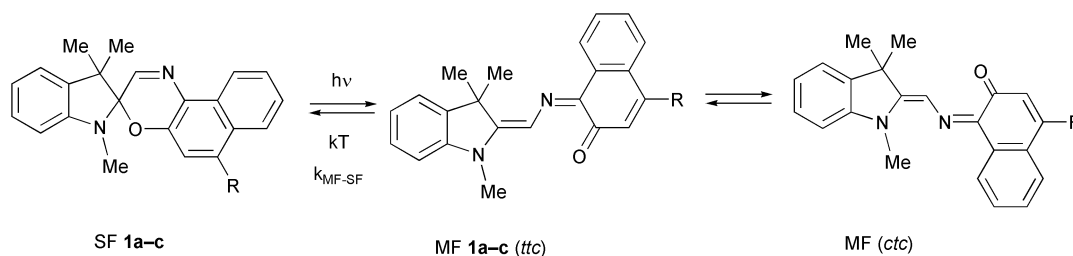


Fig. 2 Relative changes in the optical density at 380 nm for CSN **1b** in MeCN vs. the concentration of Li^+ (4), Ca^{2+} (3), Sr^{2+} (5), and Ba^{2+} (6) perchlorates, and for CSN **1c** vs. the concentration of Mg^{2+} (7), Ca^{2+} (2), and Ba^{2+} (1) perchlorates. Solid lines show the theoretical curves predicted by the model: $L + M \rightleftharpoons LM$, $K = [LM]/[L][M]$.

Table 3 The positions of proton signals in the NMR spectrum of CSN **1b** in CD₃CN and the shifts of proton signals (given in parentheses) induced by the addition of Mg(ClO₄)₂ (100-fold excess), Sr(ClO₄)₂ (10-fold excess), and Ba(ClO₄)₂ (10-fold excess)

Compound	C(Me) ₂	N-Me	H-2'	H-10'	H-9'	H-8'	H-7'	H-5'	Crown ether	
									NCH ₂	OCH ₂
1b	1.34	2.74	7.70	8.52	7.55	7.39	8.30	6.88	3.40	3.52–3.62
1b ·Mg ²⁺ (SF)	1.30	2.80	7.74	8.53	7.59	7.44	8.32	6.49	3.45	3.60–3.75
	(−0.04)	(0.04)	(0.04)	(0.01)	(0.04)	(0.05)	(0.02)	(−0.39)	(0.05)	(~0.1)
(MF)		5.44	9.93							
1b ·Sr ²⁺	1.36, 1.38	2.70	7.88	8.69	7.66	7.52	8.13	6.92	3.50	3.60–3.75
	(0.02)	(−0.04)	(0.18)	(0.17)	(0.11)	(0.13)	(−0.17)	(0.04)	(0.10)	(~0.1)
1b ·Ba ²⁺	1.34, 1.36	2.70	7.82	8.65	7.65	7.54	8.15	6.92	3.50	3.60–3.75
	(0.02)	(−0.04)	(0.12)	(0.13)	(0.10)	(0.15)	(−0.15)	(0.04)	(0.10)	(~0.1)



Scheme 3

concentration of the Mg²⁺ cations as a series of additional proton signals in the NMR spectrum. In particular, the 9.93 and 5.44 ppm signals are distinctly detected, which are typical for the azomethine proton and the N-Me group of MF,¹⁸ respectively. Hence, the differences in the proton shifts caused by the Mg²⁺ cations and those induced by the Sr²⁺ or Ba²⁺ cations can be due to the fact that Sr²⁺ and Ba²⁺ cations produce **D** complexes mainly, whereas both **D** and **F** complexes coexist in the presence of Mg²⁺ cations. In general, the results of the NMR and spectrophotometric studies of complexation are in agreement.

FTIR study of CSN **1b and its complexes with metal cations.** Under constant irradiation of an SN **1a** solution, a small steady-state concentration of the photolysis product MF appears, while most of SN **1a** remains in SF (Scheme 3). MF is identified by difference spectroscopy, which shows a new peak at 1713 cm^{−1} (Fig. 4) amongst others. CSN **1b** has a number of IR bands in the 1700 cm^{−1} region (Fig. 5) that are absent from the SN spectrum. A similar irradiation experiment with CSN **1b** also exhibits a small peak at 1710 cm^{−1} in the difference spectrum (Fig. 5). As before, SF is clearly the dominant species

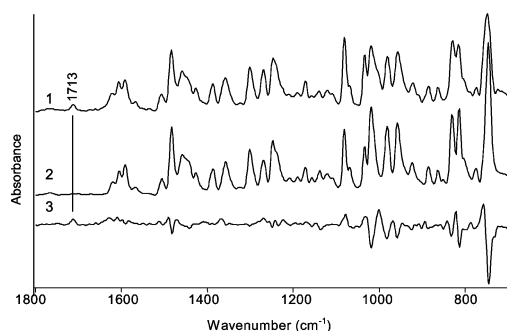


Fig. 4 FTIR spectra of SN in MeCN while undergoing irradiation at 360 nm (1), without irradiation (2) and the difference (trace 1 minus trace 2) spectrum (3). The contribution of MeCN has been subtracted.

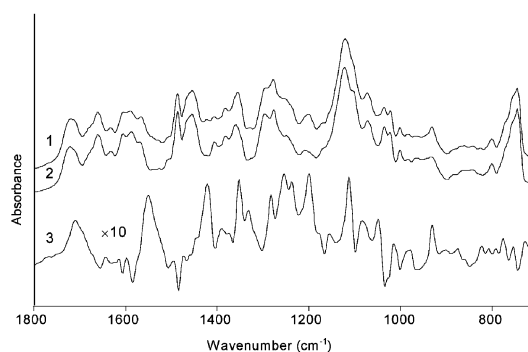


Fig. 5 FTIR spectra of CSN in MeCN while undergoing irradiation at 360 nm (1), without irradiation (2) and the difference (trace 1 minus trace 2) spectrum (3). The contribution of MeCN has been subtracted. Note that the intensity of spectrum 3 is multiplied by 10.

even under irradiation of CSN **1b** due to the fast back-reaction of MF. The irradiation-induced features at 1710–1713 cm^{−1} may be attributed to the unique C=O bond resulting in each case from the transformation of SF into MF (Scheme 3). Detection of the C=O bond vibrational mode indicates that the quinoidal, rather than hybrid resonance or zwitterionic structure, is characteristic of the photoinduced merocyanine form of both SN and CSN **1b** in acetonitrile solution.

The effect of adding a large excess of Ba²⁺ cations to a CSN **1b** solution in MeCN is shown in Fig. 6. The metal salt addition caused the solution colour to change from red to blue, indicative of the formation of metal-complexed MF. The scale-expanded difference FTIR spectrum shows a new strong band at 1726 cm^{−1} attributed to the C=O bond of the metal-complexed MF. It was also observed that the intensity of this band, and the strong feature at 1281 cm^{−1}, increased on addition of small amounts of water to the solution. This result appears to indicate that added water induces a shift in the equilibrium between the SF and MF species, probably due to water hydrogen-bonding to the C=O group, thus stabilising the MF species. The crown ether group is known to give a

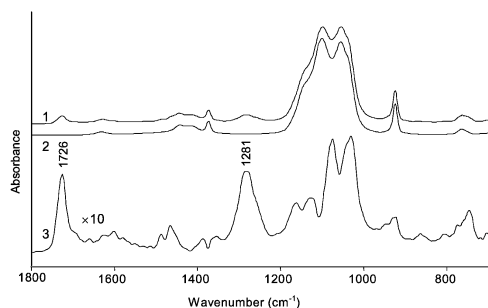


Fig. 6 FTIR spectrum of CSN in MeCN with added $\text{Ba}(\text{ClO}_4)_2$ (1), spectrum of $\text{Ba}(\text{ClO}_4)_2$ (2) and the difference (trace 1 minus trace 2) spectrum (3). The contribution of MeCN has been subtracted. The intensity of spectrum 3 is multiplied by 10.

characteristic band in the 1100 cm^{-1} region. Metal complexation appears to shift this band down into the $1000\text{--}1100\text{ cm}^{-1}$ range.

A closely similar set of experiments using $\text{Mg}(\text{ClO}_4)_2$ in place of $\text{Ba}(\text{ClO}_4)_2$ yielded similar results (Fig. 7). In particular, a new $\text{C}=\text{O}$ band was found at 1726 cm^{-1} . These experiments indicate that the quinoidal structure is preserved when MF complexes with metal cations. Two cations should be bound per molecule of CSN **1b** under the conditions used for FTIR titration, as follows from the spectrophotometry data. The first one is bound to the crown moiety, as clearly indicated in the FTIR spectra by the downward shift of the 1100 cm^{-1} band attributed to the crown group. Binding of the second cation is the main reason for MF stabilisation, and the merocyanine oxygen is a suitable site for this interaction. The interaction between the cation and the merocyanine oxygen does not lower the $\text{C}=\text{O}$ bond stretching frequency, that is it does not reduce the order of the $\text{C}=\text{O}$ bond. Therefore, coordination of the metal cation with an electron lone pair on the oxygen and, probably, also with the lone pair on the merocyanine nitrogen atom can be implied (Scheme 2, complex F). A similar complex was observed previously for crown ether containing spironaphthoxazines.¹² Consistent with the FTIR data, such an interaction evidently stabilises the quinoidal structure of MF. It should be noted that hydrogen bonding with a water molecule could also involve the electron lone pairs of the merocyanine oxygen and nitrogen atoms. In this sense, the very similar $\text{C}=\text{O}$ bond stretching frequencies of MF observed upon addition of both water molecules and metal cations are consistent with the metal-coordination model. Moreover, metallation of the crown part of the molecule will result in withdrawal of the electron lone pair on the crown nitrogen atom from conjugation with the aromatic system, and this may account for the observed 13 cm^{-1} increase in the $\text{C}=\text{O}$ bond stretching frequency on metallation.

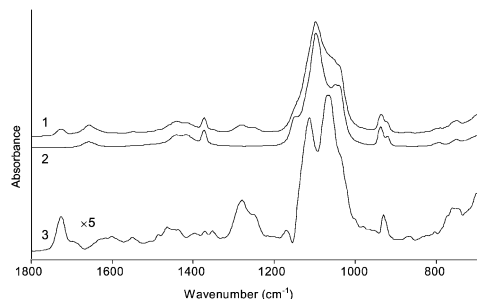


Fig. 7 FTIR spectrum of CSN in MeCN with added $\text{Mg}(\text{ClO}_4)_2$ (1), spectrum of $\text{Mg}(\text{ClO}_4)_2$ (2) and the difference (trace 1 minus trace 2) spectrum (3). The contribution of MeCN has been subtracted. The intensity of spectrum 3 is multiplied by 5.

Conformation of the merocyanine form of CSN **1b** and its complexes with Mg^{2+} cations

Features of the interaction between MF of CSN **1b** and Mg^{2+} cations were further investigated with surface-enhanced Raman scattering (SERS) spectroscopy. The SERS spectra of CSN **1b** and its complexes with Mg^{2+} cations at the C_M/C_L ratios of 1/2, 1/1, 10/1 and 100/1 are presented in the Fig. 8 and 9. As shown earlier,¹⁹ these spectra correspond to MF of the dye (spectra *a*) and complexes of this form with Mg^{2+} cations (spectra *b*–*e*). Selective SERS-assisted detection of the MF species in solution with the dominant SF is possible due to preferential MF adsorption at the SERS-active surface (this adsorption is required for realisation of the SERS effect) and a well-known resonance enhancement of the SERS signal of the coloured species. Moreover, MF seems to be stabilised due to adsorption at the silver surface, and irradiation with visible light does not induce its conversion to SF. Previously, similar prevention of light-induced trans-cis isomerization was observed for adsorbed crown ether styryl dyes and explained by fast nonradiative energy transfer from the dye excited state to the silver surface.²⁰

Interaction with a silver surface occurring upon the adsorption of CSN **1b** on the SERS-active electrode does not

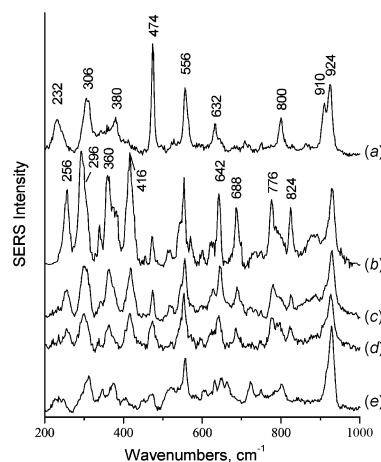


Fig. 8 SERS spectra of CSN **1b** (a) and its complexes with Mg^{2+} cations in acetonitrile at different Mg^{2+} /ligand molar ratios: 1/2 (b), 1/1 (c), 10/1 (d), 100/1 (e). The $200\text{--}1000\text{ cm}^{-1}$ range is presented.

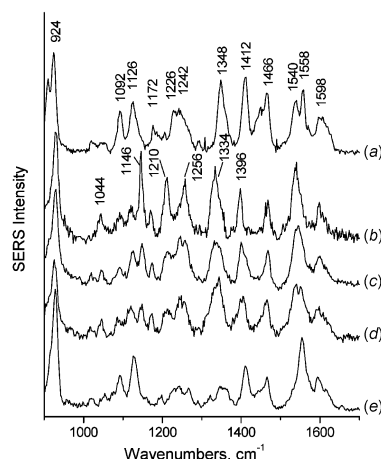


Fig. 9 SERS spectra of CSN **1b** (a) and its complexes with Mg^{2+} cations in acetonitrile at different Mg^{2+} /ligand molar ratios: 1/2 (b), 1/1 (c), 10/1 (d), 100/1 (e). The $900\text{--}1700\text{ cm}^{-1}$ range is presented.

preclude the formation of a complex with Mg^{2+} cations. Addition of Mg^{2+} cations to a CSN **1b** SERS solution induces considerable changes both in frequency and relative intensity of many SERS bands of the dye as well as the appearance/disappearance of some bands (Figs. 8, 9). These changes occur in two stages. The first stage is a drastic alteration in the spectrum of the Mg^{2+} /CSN **1b** mixture as compared to that of the free dye appearing at a low C_M/C_L ratio. The second stage changes occur with the increase in Mg^{2+} cation concentration to a 100/1 molar ratio. This two-stage process of interaction between CSN **1b** and Mg^{2+} cations is obviously related to the existence of two cation binding sites, namely, the azacrown ether moiety and the merocyanine oxygen.

Data from a UV-vis absorption study indicate that the azacrown ether cycle is a primary binding site for alkali and alkaline earth metals. This allows the SERS spectrum of the Mg^{2+} /CSN **1b** mixture recorded at the 1/2 molar ratio to be assigned to **E** (Scheme 2). Then, the spectral changes observed with an increase in the C_M/C_L ratio correspond to formation of complex **F** (Scheme 2). Direct identification of azacrown ether *vs.* merocyanine oxygen interactions from the analysis of SERS spectra is presently complicated. On the basis of a comparison of SERS spectra of model compounds (indoline base and 1,2-naphthoquinone containing aza-15-crown-5 ether in the 4-position) and structurally similar derivatives (SN **1a**, 6'-morpholinospironaphthoxazine) it was concluded that the bands of both naphthalene and indolinic moieties are present in the CSN **1b** spectrum, and some of them were coupled because of considerable conjugation of both chromophores.¹⁹ At the same time vibrations of the crown ether moiety were not enhanced, since they are not in resonance with the electronic transition. The 1532 and 1554 cm^{-1} bands were assigned to the coupled double bond stretching mode of the conjugated polyene-like chain of CSN **1b**. It was concluded that two isomers of CSN **1b** differing in conformation of the $=\text{C}-\text{N}=\text{C}$ bridge coexist in solution. These are the *trans-trans-cis* (*ttc*) and *cis-trans-cis* (*ctc*) conformers (Scheme 3) represented in the SERS spectrum by the 1532 and 1554 cm^{-1} bands, respectively.

The disappearance of the 1554 cm^{-1} band in the Mg^{2+} /CSN **1b** spectrum at low C_M/C_L ratio (Fig. 9, spectrum *b*) allows one to conclude that Mg^{2+} binding to the azacrown ether moiety stabilises the single *ttc* isomer in solution. Relative enhancement of the 1554 cm^{-1} band with an increase in the C_M/C_L ratio (Fig. 9, spectra *c*, *d*) manifests itself as *ctc* isomer formation induced by the interaction of the Mg^{2+} cation with the merocyanine oxygen. The presence of the single 1554 cm^{-1} band in the spectrum of Mg^{2+} /CSN **1b** at a 100/1 molar ratio (Fig. 9, spectrum *e*) shows that the *ctc* isomer dominates, when two Mg^{2+} cations are bound to CSN **1b**.

It should be noted that under the same conditions it was impossible to detect stabilisation of the single *ttc* isomer of CSN **1b** upon addition of Ba^{2+} or Ca^{2+} cations (data not shown). The spectral changes are observed at the 10/1–100/1 molar ratios. The spectra are very similar to that of Mg^{2+} /CSN **1b** at a 100/1 molar ratio and indicated the stabilisation of the *ctc* isomer.

These MF isomerisation properties of CSN **1b** are considerably different from those of SN **1a**. The *ab initio* MO and ^1H NMR NOE studies revealed that the *ttc* and *ctc* isomers were most stable among the probable MF isomers of SN **1a**.²¹ The *ttc* isomer was calculated to be slightly more stable than the *ctc* one. A SERS spectroscopy study revealed that a single isomer (*ttc* according to Nakamura *et al.*²¹) was observed for free MF of SN **1a** and its complexes with metal cations. Therefore, the appearance of two MF isomers, which is a property of both CSN **1b** and the 6'-morpholine derivative of SN **1a**,¹⁹ is closely associated with the introduction of an electron-donating substituent. Results presented here show that the cation-induced MF isomerisation is an additional feature of CSN **1b**.

Thermal relaxation of photoinduced MF of CSN **1b,c** and their complexes with metal cations

Similarly to unsubstituted SN **1a** the spiro form of CSN **1b,c** undergoes a UV-light-induced reversible isomerisation to coloured MF, which relaxes spontaneously back to SF (Scheme 3). The introduction of an azacrown ether fragment increases sixfold the rate constant for the thermal relaxation of the coloured form of CSN **1b,c** with respect to the same parameter of SN **1a** (Table 1). This effect is typical for electron-donating substituents.²²

The rate constant for the thermal relaxation ($k_{\text{MF} \rightarrow \text{SF}}$, Scheme 3) of the photoinduced MF of SN **1a** and CSN **1b,c** tends to gradually decrease upon addition of metal cations and with increasing metal concentration (Fig. 10). Binding of metal cations to the open oxazine ring of MF is evidently the main reason from the slowed relaxation of SN **1a** to the spiro form. The same reason can explain a decrease of $k_{\text{MF} \rightarrow \text{SF}}$ for CSN **1b,c** at high C_M/C_L ratios, when the dependence of $k_{\text{MF} \rightarrow \text{SF}}$ on the C_M/C_L ratio is rather similar for SN **1a** and CSN **1b,c**. This is realised for Mg^{2+} (Fig. 10, A) and, especially, Ca^{2+} (Fig. 10, B) cations. The presence of the azacrown ether moiety disrupts this similarity at the low C_M/C_L ratios, and the ability of the cation to bind to the azacrown ether cycle plays an important role here. Thus, due to high affinity binding of Ca^{2+} and Ba^{2+} cations to the azacrown ether moiety of CSN **1c** (Table 2), the $k_{\text{MF} \rightarrow \text{SF}}$ values decrease sharply at low C_M/C_L ratios (Fig. 10, B, C). The effect of this interaction seems to dominate the influence of cation binding to the open oxazine ring up to moderate C_M/C_L ratios. A plateau in the dependence of $k_{\text{MF} \rightarrow \text{SF}}$ on the C_M/C_L ratio appears when the cation binding to the azacrown ether moiety saturates, but remains the rate-determining factor of thermal relaxation. The interaction between the metal ions and the azacrown ether moiety in the **E** complex reduces the electron-donating properties of the azacrown ether fragment and thus decreases the electron density on the merocyanine oxygen atom. This effect hampers the ring-closure reaction and SF formation. This explanation is in line with the variations of the rate constant caused by the introduction of electron-donating and electron-withdrawing substituents at the 6-position of SN **1a** reported in the literature.²²

It should be mentioned that at low Mg^{2+} concentrations ($C_M/C_L = 1\text{--}10$), $k_{\text{MF} \rightarrow \text{SF}}$ of CSN **1b** is larger than $k_{\text{MF} \rightarrow \text{SF}}$ of CSN **1b** without metal cation (Fig. 10, A). According to the SERS spectroscopic data (see above), binding of a Mg^{2+} cation (but not Ba^{2+} or Ca^{2+} cations) with the azacrown ether cavity stabilises the single *ttc* isomer, instead of the two *ttc* and *ctc* isomers that are characteristic of free MF (Scheme 3).

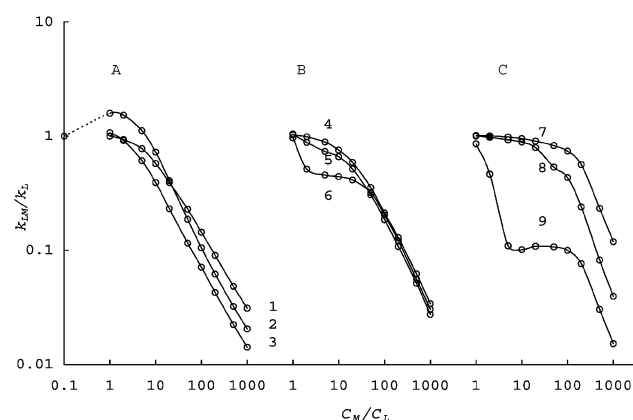
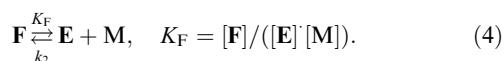


Fig. 10 Relative $k_{\text{MF} \rightarrow \text{SF}}$ of MF of SN **1a** (1,4,7), CSN **1b** (2,5,8), CSN **1c** (3,6,9) *vs.* the concentrations of Mg^{2+} (A), Ca^{2+} (B) and Ba^{2+} (C) perchlorates.

Obviously, the relaxation of photoinduced MF to SF is facilitated for the *ttc* isomer as compared to the *ctc* isomer, increasing the $k_{\text{MF} \rightarrow \text{SF}}$ value. In turn, the appearance of the *ctc* isomer with an increase in the $C_{\text{M}}/C_{\text{L}}$ ratio (see above) contributes to the decrease of the $k_{\text{MF} \rightarrow \text{SF}}$ value.

In accordance with the above consideration a general pathway of thermal relaxation of photoinduced MF at $C_{\text{M}}/C_{\text{L}} > 100$ can be represented as follows: $\text{F} \rightarrow \text{E} \rightarrow \text{D}$ (Scheme 2). Here it is assumed that the efficiency of metal cation interaction with the azacrown ether moiety is considerably higher than that with the open oxazine ring, and SF formation occurs *via* thermal dissociation of the metal cation bound to the open oxazine ring. In this case, the kinetic data can be analysed in terms of the model



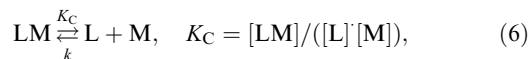
The rate constant k for deactivation of complex **F** measured experimentally is determined by the relation

$$k = (k_1 + k_2 K_{\text{F}}[\text{M}]) / (1 + K_{\text{F}}[\text{M}]) \quad (5)$$

where k_1 , k_2 are the rate constants for deactivation of **E** and **F**, and K_{F} is the equilibrium constant of process (4). This scheme is similar to that proposed previously²³ for the complexation of spiro compounds without crown ether fragments.

However, even at high $C_{\text{M}}/C_{\text{L}}$ ratios the experimental data for thermal relaxation of CSN **1b,c** agree with the theoretical curves plotted using eqn. (5) only for Ca^{2+} cations. The calculated K_{F} values are presented in the Table 2. As assumed, they are markedly lower than the corresponding complexation constants involving the azacrown ether fragment of SF (Table 2).

The scheme for thermal relaxation of SN **1a** is simplified:



where K_{C} is the equilibrium constant of complexation between SN **1a** and metal cations. The experimental data for thermal relaxation of SN **1a** agree with the theoretical curves plotted using eqn. (6), and the K_{C} value for Ca^{2+} cations is presented in Table 2. It should be noted that the K_{F} constants for CSN **1b,c** and the K_{C} constant for SN **1a** are rather similar in the case of complexation with Ca^{2+} cations.

Conclusions

The synthesis and study of spironaphthoxazines conjugated with aza-15(18)-crown-5(6)-ether fragments were performed for the first time. It was demonstrated that the introduction of an azacrown ether into the spironaphthoxazine structure induces changes in the spectral and photochemical properties of SF similar to those resulting from the introduction of an electron-donating substituent, for example, a morpholine or piperidine residue. The addition of alkaline earth metal cations to solutions of CSN **1b,c** alters the characteristics of the photoinduced transformation and results in changes of the absorption spectra of both SF and MF. The complex formation process of CSN **1b,c** with Li^+ and alkaline earth metal cations in MeCN involves two probable sites: the crown ether centre and the merocyanine oxygen in the naphthalene part of the molecule. At $C_{\text{M}}/C_{\text{L}}$ molar ratios ranging from 1 to 100, the formation of complexes occurs with participation of the crown ether fragment of the molecule, whereas the participation of the merocyanine oxygen atom in complex formation is possible at high metal cation concentration ($C_{\text{M}}/C_{\text{L}} > 100$). The correspondence between the crown cavity and the metal

cation sizes is important for efficient binding. The stability of the complex formed by interaction of the merocyanine oxygen atom with a metal cation depends on the charge density of the metal cation. It was found that the strength of the ‘‘crown ether–metal cation’’ complexes of SF is higher than those involving MF by more than two orders of magnitude. The study of these compounds is important as regards the search for new types of materials whose spectral and photochromic properties are highly sensitive to the metal cations present in solution.

Experimental

Instrumental analysis

^1H NMR spectra were recorded on Bruker AMX-400 and Bruker DRX-500 spectrometers using TMS as the internal standard and CD_3CN as the solvent. The chemical shifts and the spin-spin coupling constants were determined with an accuracy of 0.01 ppm and 0.1 Hz, respectively. Mass spectra were obtained using a Varian MAT 311A instrument with an ionisation energy of 70 eV. The reactions were monitored by TLC on DC-Alufolien Kieselgel 60 F_{254} (Merck) plates. For column chromatography, silica gel 60 with a particle size of 0.063–0.200 mm was used.

Optical investigations

Electronic absorption spectra were measured on a Shimadzu UV-3100 spectrophotometer. The electronic absorption spectra of MF were recorded using a spectrophotometric setup with continuous irradiation of samples by a DRSh-250 mercury lamp at 365 nm.

The kinetics of the thermal relaxation of MF were measured using a kinetic setup in the time range of 0.001–1000 s. The chromophores were photoexcited by exposure to the UV radiation of a pulse xenon lamp. The measurements were performed in solution at a ligand concentration $C_{\text{L}} = 0.2 \text{ mM}$ and a temperature of 298 K. Acetonitrile (Aldrich, water content 0.005%) was used as a solvent. The analytical grade lithium, magnesium, calcium, strontium, and barium perchlorates were used for the investigations without additional purification.

FTIR investigations

FTIR spectra were obtained using a Mattson-Unicam instrument with a DuraSamplIR ATR sample unit fitted with a 3-reflection Si/ZnSe DuraDisk (Spectroscopy Central, UK). The 128 scans were routinely accumulated at 8 cm^{-1} resolution. A medium pressure Hg lamp (Philips, model HPK, 125 W) fitted with a Schift glass filter and an H_2O filter to produce an output beam centered at 368 nm was used for photolysis. Concentrated solutions of SN and CSN were prepared in pure dry acetonitrile. Anhydrous BaClO_4 and MgClO_4 were added in excess to CSN solutions.

SERS investigations

An acetonitrile solution of CSN **1b** (0.2 mM) was titrated with magnesium perchlorate (0.1–20 mM) and studied with SERS spectroscopy. SERS spectra were measured for the dye and its complexes with Mg^{2+} cations adsorbed on an electrochemically roughened silver electrode. The silver electrode was used as a SERS-active substrate as being stable to organic solvents and different ion compositions. It was prepared for SERS experiments as follows. The silver electrode was polished, boiled in 0.1 M NaOH, washed with triply distilled water and subjected to an oxidation-reduction cycle in the

aqueous electrolyte solution (0.1 M KCl) with a standard electrochemical cell. Roughened in this way the electrode was washed with triply distilled water, dried and washed again with acetonitrile to remove electrolyte and water traces. After this the electrode was placed in a glass cell with the solution under study. SERS measurements were performed at an undefined potential. SERS spectra were recorded with a Ramanor HG-2S spectrometer (Jobin Yvon, France) in the 200–1800 cm⁻¹ range (1 cm⁻¹ increment, 1 s integration time) and averaged over 3 scans. Excitation wavelength was 647.1 nm of a Kr ion laser (Spectra-Physics, Model 164–03). Laser power was 20 mW.

Ligand synthesis

The crown-containing spironaphthoxazines were synthesised using 1,3,3-trimethyl-2-methyleneindoline (Fluka), aza-15-crown-5 and aza-18-crown-6 (Merck), and 1-nitroso-2-naphthol, the sodium salt of 4-sulfo-1,2-naphthoquinone, and methyl alcohol (Aldrich). The chemicals were used as received.

1,3,3-Trimethyl-6-(1,4,7,10-tetraoxa-13-azacyclopentadec-13-yl)spiro[indolino-2,3'-[3H]naphtho[2,1-b]oxazine} (1b) by method A. 1-Nitroso-2-naphthol (0.393 g, 2.25 mmol) was added to a solution of of aza-15-crown-5 ether (1 g, 4.6 mmol) in MeOH (5 ml). The mixture was heated under argon for 6 h at 80 °C, and 1,3,3-trimethyl-2-methyleneindoline (0.4 ml, 2.25 mmol) dissolved in MeOH (10 ml) was added. The reaction mixture was allowed to rest for 2.5 h at 80 °C, cooled, and concentrated. Column chromatography repeated two times yielded 0.43 g (47%) of compound **1a**²⁴ and 26 mg (6%) of compound **1b**. ¹H NMR (DMSO-d₆, δ , J/Hz): 1.34 (s, 6H, 2CH₃); 2.74 (s, 3H, NCH₃); 3.20–3.70 (m, 20H, 2NCH₂+4OCH₂); 6.63 [d, 1H, H(7), $J=7.8$]; 6.85 [t, 1H, H(5), $J=7.5$, $J=7.5$]; 6.90 [s, 1H, H(5')]; 7.13 [m, 2H, H(4), H(6)]; 7.35 [t, 1H, H(8'), $J=6.9$, $J=8.0$]; 7.50 [t, 1H, H(9'), $J=7.9$, $J=7.2$]; 7.71 [s, 1H, H(2')]; 8.31 [d, 1H, H(7'), $J=8.1$]; 8.51 [d, 1H, H(10'), $J=8.4$]. Anal. found (%): C, 70.83; H, 7.46; N, 7.05. Calcd (%) for C₃₂H₃₉N₃O₅: C, 70.43; H, 7.20; N, 7.70.

1,3,3-Trimethyl-6-(1,4,7,10,13-pentaoxa-17-azacyclohexadodec-17-yl)spiro[indolino-2,3'-[3H]naphtho[2,1-b]oxazine} (1c) by method A. This compound was prepared in a similar way from aza-18-crown-6 ether. Yield 3%. ¹H NMR (DMSO-d₆, δ , J/Hz): 1.34 (s, 6H, 2CH₃); 2.74 (s, 3H, NCH₃); 3.52 (m, 20H, 2NCH₂+4OCH₂); 6.63 [d, 1H, H(7), $J=7.8$]; 6.85 [t, 1H, H(5), $J=7.8$, $J=7.1$]; 6.95 [s, 1H, H(5')]; 7.1–7.19 [m, 2H, H(4), H(6)]; 7.35 [t, 1H, H(8'), $J=6.9$, $J=8.4$]; 7.50 [t, 1H, H(9'), $J=7.4$, $J=7.2$]; 7.71 [s, 1H, H(2')]; 8.15 [d, 1H, H(7'), $J=8.3$]; 8.51 [d, 1H, H(10'), $J=8.1$]. Anal. found (%): C, 68.44; H, 6.64; N, 6.72. Calcd (%) for C₃₄H₄₃N₃O₆·0.5 CH₃OH: C, 68.40; H, 7.48; N, 6.93.

4-(1,4,7,10-Tetraoxa-13-azacyclopentadec-13-yl)-1,2-naphthoquinone (2) by method B. A mixture of the sodium salt of 4-sulfo-1,2-naphthoquinone (1 g, 4 mmol) and aza-15-crown-5 ether (1 g, 4.6 mmol) was dissolved in 30 ml of water and stirred for 6 h at room temperature. At the end of the reaction, the mixture was extracted into chloroform, the solvent was evaporated, and the residue was recrystallised from ether. The yield of **2** was 0.46 g (31%), m.p. 131–146 °C. ¹H NMR

(CD₃CN-d₃, δ , J/Hz): 2.82 [m, 4H, N(CH₂)₂]; 3.15 (m, 8H, 4OCH₂); 3.28 (t, 2H, OCH₂); 3.90 (t, 2H, OCH₂); 6.1 [s, 1H, H(3)]; 7.50 [t, 1H, H(6), $J=7.5$, $J=7.5$]; 7.6 [t, 1H, H(7), $J=7.5$, $J=7.8$]; 7.83 [d, 1H, H(5), $J=7.8$]; 8.08 [d, 1H, H(8), $J=7.8$]. MS: m/z ($I_{\text{rel.}}/\%$) 377 ([M⁺], 7); 216 (59); 173 (100); 172 (87); 171 (41); 159 (83); 158 (85); 145 (37); 129 (62); 115 (42).

Acknowledgements

This work was supported by the Russian Foundation for Basic Research (grant No. 02-03-33058), PICS (grant No. 705), and INTAS (grant No. 97-31193).

References

- 1 R. C. Bertelson, *Photochromism, Techniques in Chemistry*, ed. G. H. Brown, Wiley Interscience, New York, 1971, vol. 3, p. 45.
- 2 R. Guglielmetti, *Photochromism-Molecules and Systems Studies in Organic Chemistry*, ed. H. Durr and H. Bouas-Laurent, Elsevier, Amsterdam, 1999, vol. 40, p. 314.
- 3 V. A. Barachevsky, *Spectroscopy of Phototransformations in Molecules*, ed. A. A. Krasnovsky, Leningrad, 1977, p. 182.
- 4 L. Cazaux, M. Fajer, A. Lopez, C. Picard and P. Tisnes, *J. Photochem. Photobiol., A*, 1994, **77**, 217.
- 5 J. Bourson, F. Badaoui and B. Valeur, *J. Fluoresc.*, 1994, **4**, 275.
- 6 A. P. de Silva and K. R. A. S. Sandanayake, *Angew. Chem., Int. Ed. Engl.*, 1990, **29**, 1173.
- 7 S. Das, G. K. Thomas, K. Y. Thomas, P. V. Kamat and M. V. George, *J. Phys. Chem.*, 1994, **98**, 9291.
- 8 S. P. Gromov and M. V. Alfimov, *Russ. Chem. Bull.*, 1997, **46**, 611.
- 9 M. Inouye, M. Ueno, K. Tsuchiya, N. Nakayama, T. Konishi and T. Kitao, *J. Org. Chem.*, 1992, **57**, 5377.
- 10 V. B. Nazarov, V. A. Soldatenkova, M. V. Alfimov, P. Lareginie, A. Samat and R. Guglielmetti, *Russ. Chem. Bull.*, 1996, **45**, 2220.
- 11 O. A. Fedorova, S. P. Gromov, Y. V. Pershina, S. A. Sergeev, Y. P. Strokach, V. A. Barachevsky, M. V. Alfimov, G. Pepe and A. Samat, *Russ. Chem. Bull.*, 1999, **48**, 1950.
- 12 O. A. Fedorova, S. P. Gromov, Y. V. Pershina, S. A. Sergeev, Y. P. Strokach, V. A. Barachevsky, M. V. Alfimov, G. Pepe, A. Samat and R. Guglielmetti, *J. Chem. Soc., Perkin Trans 2*, 2000, 563.
- 13 M. Rickwood, S. D. Marsden, M. E. Ormsby, A. L. Staunton, D. W. Wood, J. D. Hepworth and C. D. Gabbut, *Mol. Cryst. Liq. Cryst.*, 1994, **246**, 17.
- 14 Y. P. Strokach, V. A. Barachevsky, M. V. Alfimov, G. Pepe, A. Samat and R. Guglielmetti, *Zh. Nauchn. Prikl. Fotogr.*, 1999, **44**, 1.
- 15 J. Bourson, J. Pouget and B. Valeur, *J. Phys. Chem.*, 1993, **97**, 4552.
- 16 *Handbook of Chemistry and Physics*, ed. R. C. Weast, CRC Press, Boca Raton, FL, 66th edn., 1985, p. F-164.
- 17 *Host-Guest Chemistry*, eds. F. Vogtle, E. Weber, Marcel Dekker, New York, 1981.
- 18 R. L. Zaitchenko, F. V. Lubimov, V. S. Marevtsev and M. I. Cherkashin, *Russ. Chem. Bull.*, 1988, **37**, 1040.
- 19 A. V. Feofanov, Y. S. Alaverdian, S. P. Gromov, O. A. Fedorova and M. V. Alfimov, *J. Mol. Struct.*, 2001, **563–564**, 193.
- 20 A. Feofanov, A. Ianoul, V. Oleinikov, S. Gromov, O. Fedorova, M. Alfimov and I. Nabiev, *J. Phys. Chem. B*, 1997, **101**, 4077.
- 21 S. Nakamura, K. Uchida, A. Murakami and M. Irie, *J. Org. Chem.*, 1993, **58**, 5543.
- 22 *Organic Photochromic and Thermochromic Compounds*, eds. J. C. Crano and R. Guglielmetti, Plenum Press, New York, 1999.
- 23 J.-W. Zhou, Y.-T. Li and X.-Q. Song, *J. Photochem. Photobiol. A: Chem.*, 1995, **87**, 37.
- 24 H. Ono and C. Osada, *GB Pat.*, 1970, 1,186,987.